CRYSTALLIZATION IN COLLOIDAL SUSPENSIONS

J. S. VAN DUIJNEVELDT AND H. N. W. LEKKERKERKER
Van 't Hoff Laboratory, Utrecht University
Padualaan 8, 3584 CH Utrecht, The Netherlands

Abstract. The use of colloidal suspensions as model systems to study crystallization is briefly reviewed. It is shown how the classical theories of crystal nucleation and crystal growth can be applied to colloidal hard-spheres. Predictions are compared with experimental observations.

1. Introduction

Suspensions are called colloidal when the size of the suspended particles is between 1 nm and 1 μm. On the one hand, these particles are larger than atoms or small molecules. On the other hand, the particles are sufficiently small to undergo vivid Brownian motion, due to interactions with solvent molecules, and sedimentation is generally slow, if it occurs at all. More specifically, we shall consider suspensions of monodisperse spherical particles with a diameter σ ranging from $0.2 - 1$ μm. Like atomic systems, such suspensions can undergo crystallization, resulting in a regular spatial arrangement of the particles. We briefly review the use of such suspensions as models to study crystallization. The main part of this contribution consists of an attempt to adapt the classical theories of crystal nucleation and crystal growth to describe the crystallization kinetics in suspensions of colloidal hard-spheres.

Colloidal suspensions have several properties that render them suitable as model systems for studying crystallization. First of all, it should be noted that colloidal suspensions are thermodynamically equivalent to atomic systems [1,2]. Thermodynamic properties of an atomic system can be calculated using statistical mechanics, starting from the interaction potential. The same can be done for a colloidal suspension, when instead of the bare interaction potential between colloidal particles the potential of mean force is used, in which the forces exerted by the solvent molecules are taken into account. Therefore, colloidal suspensions
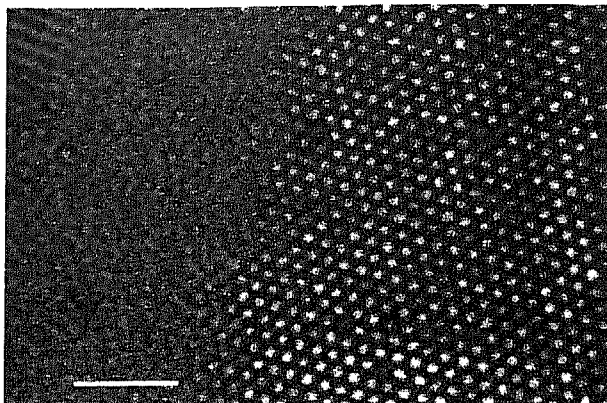
279

Figure 1. CSLM graph of two colloidal crystals in equilibrium with a colloidal fluid. Average of ten scans ($\sim$ 10 s). Silica particles ($\sigma = 430$ nm) with a fluorescent core, coated with stearyl alcohol and dispersed in chloroform. These particles are somewhat charged and crystallize at $\phi = 0.07$ (bar 5 μm). Reprinted with permission from Ref. [3]. Copyright 1994 American Chemical Society.

can serve as models for atomic systems.

The size of colloidal particles has a number of consequences. Firstly, it allows suspensions to be studied conveniently with experimental techniques such as light scattering and light microscopy. An example of two colloidal crystals in coexistence with a colloidal fluid is shown in Figure 1. This micrograph has been made using fluorescence confocal scanning laser microscopy (CSLM), from a dispersion of silica particles with a fluorescent core [3]. In the fluid phase the particles are blurred because significant diffusion occurs during the observation time ($\sim$ 10 s).

Secondly, colloidal crystals are very weak. A measure for the strength of a material is the bulk modulus, which we estimate as $\mathcal{K} \sim k_B T \sigma^{-3}$, where $k_B T$ is the thermal energy. A colloidal particle being about a thousand times larger than an atom, the bulk modulus is roughly smaller by a factor of 10^9 for a colloidal crystal. As a consequence of this, external fields such as the gravitational field have an important effect on such crystals. Shearing a colloidal crystal, by shaking the sample, is often sufficient to *shear melt* the crystal.

Thirdly, dynamics are much slower in colloidal systems. A measure for this is the "structural relaxation time", expressed as $\tau_R = D/\sigma^2$, where D is a self-diffusion coefficient. It gauges the time needed for a particle to diffuse over a distance equal to its own diameter. This time scale is again much larger for a colloidal fluid compared to an atomic fluid, roughly by a factor 10^9. As a result, once a metastable fluid has been created by shear melting a crystal, recrystallization typically takes place on a time scale > 1 s. Therefore, all stages of crystal formation (nucleation, growth, and ageing) are, in principle, amenable to direct observation.

Also it is easy to prepare long-lived amorphous (glassy) states.

Finally, particle interactions, ranging from very soft interactions to hard-sphere behaviour, can be tuned by chemical modification of the particle surface and by changing the solvent. A popular model system consists of polystyrene spheres, suspended in water. Due to the presence of ionizable groups on the particle surface, these particles are charged and have a soft, long-ranged repulsive interaction. At low ionic strength body-centered-cubic (bcc) crystals are formed, whereas face-centered-cubic (fcc) crystals may be obtained if the electrostatic interactions are sufficiently screened off by adding salt. At the other end of the spectrum we find particles with a harshly repulsive interaction. The experiments we discuss below have been performed using polymethylmethacrylate (PMMA) particles, sterically stabilized by chains of poly-12-hydroxystearic acid. Suspended in a solvent such as decalin, these particles behave as colloidal hard-spheres. These particles crystallize into close-packed structures. Although fcc is believed to be the stable crystal structure, structures showing a somewhat disordered stacking of close-packed crystal planes have also been observed [4]. For a more detailed discussion of colloidal crystals, and experimental techniques to study them, the reviews by Pieranski [5], Pusey [6], and Sood [7] can be consulted.

In the remainder we shall focus on crystallization in suspensions of hard-sphere colloidal particles. The hard-sphere interaction potential is given by

$$\mathcal{V}(r) = \infty,\ r < \sigma;$$
$$\mathcal{V}(r) = 0,\ r \geq \sigma.$$

Whereas for atomic systems temperature usually is the parameter that controls crystallization, for hard spheres the control parameter is the volume fraction $\phi = \pi\sigma^3\rho/6$, where ρ is the particle number density. Using computer simulations, such particles have been shown to crystallize into an fcc lattice on increasing density [8] and the coexistent phases are at $\phi_F = 0.494$ and $\phi_M = 0.545$ [9].

Experimental observations of hard-sphere dispersions [10] show that the concentration range where crystallization is observed is very narrow, and that crystallization proceeds fastest near ϕ_M, the melting volume fraction. At higher volume fraction the particle diffusion slows down. Homogeneous crystal nucleation subsequently ceases at a certain volume fraction. Recent work on hard-sphere dispersions by van Megen and Underwood shows that this occurs at the glass transition volume fraction ($\phi_G = 0.58$), above which dynamic light scattering shows that the structure is arrested [11]. For $\phi > \phi_G$ crystal growth is still found to proceed, however.

Our aim is to construct a model to describe nucleation and growth of colloidal crystals. This model has been presented in more detail in Ref. [12]. We follow the approaches by Pusey [6] and by Russel [13], where the particle dynamics are expressed in terms of self diffusion coefficients, and therefore we first discuss the behaviour of these coefficients in colloidal suspensions in Section 2. In Section

3 the classical theories for crystal nucleation and for crystal growth are adapted to describe the behaviour of colloidal particles. In Section 4 the theory is applied to hard spheres and results are compared with experimental data. Finally, some limitations of the approach presented here are discussed.

2. Diffusion

Although there is a thermodynamic analogy between atomic systems and colloidal suspensions, there is an important difference in the description of the dynamics for the two types of system. For atomic systems the dynamics follow from Newton's laws of motion. Characteristic of colloidal suspensions is that the colloidal particles are much larger (and have a much larger mass) than the solvent molecules. Therefore, the solvent degrees of freedom relax on a much shorter time scale than those of the colloidal particles. Due to interactions with solvent molecules the velocity fluctuations of the colloidal particles decay on a time scale over which the particles move only a distance that is a fraction of their own size. This results in a diffusive (Brownian) motion of the colloidal particles [6]. The mean squared displacement $\langle (\Delta R)^2 \rangle$ as a function of time t for a sphere at infinite dilution is given by

$$\langle (\Delta R)^2 \rangle = 6D_0 t, \tag{1}$$

where D_0 is the Stokes-Einstein diffusion coefficient,

$$D_0 = \frac{k_B T}{3\pi \eta \sigma}, \tag{2}$$

with η the solvent viscosity. At finite volume fraction ϕ of colloidal particles, distinction can be made between the collective diffusion coefficient, D_c, and the self diffusion coefficient, D_s. The collective diffusion due to concentration gradients is described by D_c, whereas D_s describes $\langle (\Delta R)^2 \rangle$ for a selected particle.

Below we express the dynamics of colloidal particles in terms of D_s to estimate the rates of crystal nucleation and growth. Therefore we will first examine in more detail this self diffusion coefficient. Different behaviour is observed at short times, when particles have moved a small distance compared to σ, and at longer times. At short times a particle only experiences the presence of other particles through hydrodynamic interactions, whereas at longer times also direct particle interactions become important. These two time regimes are treated separately. For a detailed discussion of this matter see Ref. [6].

2.1. SHORT-TIME SELF DIFFUSION

To first order in ϕ, the short-time self diffusion coefficient, D_s^S, is calculated to be given by [14,15]
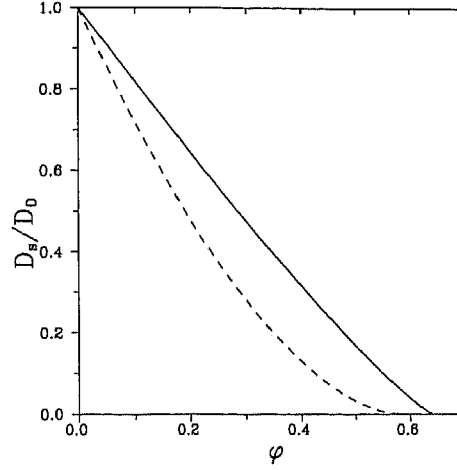
$$D_s^S = D_0(1 - 1.83\phi). \tag{3}$$

Figure 2. Comparison of our empirical expressions for D_s^S (Eq. (4), solid line) and D_s^L (Eq. (6) with $\phi_c = 0.58$ and $\delta = 1.74$, dashed line).

Estimates have been provided for the second-order term [16]. These results are supported by experiments [17,18]. For the description of crystallization, however, it is necessary to have an expression for D_s^S at high ϕ, where the fluid is in fact metastable. Following Russel [13], we assume that $D_s^S \rightarrow 0$ as $\phi \rightarrow \phi_{rcp}$, the volume fraction at random close packing ($\phi_{rcp} = 0.64$ [19]). We choose an expression of the type

$$D_s^S = D_0(1 - \phi/\phi_{rcp})^\beta.$$ (4)

Imposing the low-density limit, Eq. (3), yields an exponent $\beta = 1.17$.

2.2. LONG-TIME SELF DIFFUSION

To first order in ϕ, the long-time self diffusion coefficient, D_s^L, has been calculated to be [20,21]

$$D_s^L = D_0(1 - 2.10\phi).$$ (5)

Again little is known about the behaviour at high ϕ, where crystallization occurs. Supported by experimental studies [22,23] we again choose an expression of the form

$$D_s^L = D_0 [1 - \phi/\phi_c]^\delta.$$ (6)

Assuming $D_s^L \rightarrow 0$ at the glass transition, we put $\phi_c = \phi_G = 0.58$ [24]. The experimental data could be represented reasonably well, over the whole volume fraction range, with Eq. (6) putting $\delta = 3\phi_c = 1.74$. In Figure 2 our empirical expressions for D_s^S and D_s^L are compared. Note that both coefficients are much smaller than D_0 at $\phi > 0.5$, where crystallization occurs.

3. Nucleation and growth of crystals

In this section some results from the classical theories for homogeneous crystal nucleation and for crystal growth are adapted to describe crystallization in colloidal suspensions.

3.1. NUCLEATION

We wish to calculate I, the rate of formation of nuclei per unit volume. In order to do so we apply classical nucleation theory, in the form proposed by Turnbull and Fisher for crystallization from the melt [25]. We express their result for the steady-state nucleation rate as

$$I = f\rho \exp(-\Delta G_m/k_B T), \tag{7}$$

where f is the transition rate for a particle in contact with the crystal nucleus to become part of the nucleus, and ΔG_m is the free energy needed for creation of the (spherical) critical nucleus, given by

$$\Delta G_m = \frac{16\pi\gamma^3 v^2}{3(\Delta\mu)^2}. \tag{8}$$

Here γ is the surface free energy per unit surface between the liquid and the solid, assumed equal for all exposed crystal planes, v is the volume per particle in the solid phase, and $\Delta\mu$ is the chemical potential difference between the two phases (note that $\Delta\mu < 0$ means crystallization will proceed). The number of particles in the critical nucleus, n_m, follows from

$$n_m = \frac{32\pi\gamma^3 v^2}{3|\Delta\mu|^3}. \tag{9}$$

In order to adapt Eq. (7) to crystallization in a colloidal suspension, it is assumed that the incorporation of particles into the nucleus is a diffusive process. Therefore f is estimated as

$$f = \frac{D_s}{l^2}, \tag{10}$$

where D_s is a self diffusion coefficient and l a typical distance over which diffusion has to take place. Previously we mentioned the observation that homogeneous nucleation seems to be arrested at the glass transition, where we assume that $D_s^L \rightarrow 0$ [11]. In view of these results it seems natural to choose $D_s = D_s^L$. The latter is calculated from Eq. (6) with $\phi_c = 0.58$ and $\delta = 1.74$. Estimating the characteristic diffusion distance as

$$l = \sigma\phi^{-1/3}, \tag{11}$$

Eq. (7) now becomes

$$I = \mathcal{A}\phi^{5/3}\frac{D_s^L}{\sigma^5}\exp(-\Delta G_m/k_BT),\tag{12}$$

where we have introduced the prefactor $\mathcal{A}$. According to the brief derivation given here $\mathcal{A} = 6/\pi$. However, for atomic systems both theoretical and experimental results for $\mathcal{A}$ vary rather much and therefore it is by no means obvious that $\mathcal{A} = \mathcal{O}(1)$ (see, for instance, Ref. [26]). The same expression for I was proposed previously by Russel [13].

3.2. GROWTH

To calculate the growth rate of crystals we use the theory of Wilson [27] and Frenkel [28]. This theory describes the so-called normal growth, where it is assumed that growth can take place at any surface site. This requires that the interface is rough, which is probably justified for the colloidal suspensions discussed here (see also Fig. 1). The result for the net growth rate of a crystal, v, is given by

$$v = v_m\left[1 - \exp(\Delta\mu/k_BT)\right].\tag{13}$$

In this expression the prefactor v_m gives the maximum rate at which particles can be incorporated into the crystal, and the term $[1 - \exp(\Delta\mu/k_BT)]$ gives the "sticking probability" that a particle will actually become part of the crystal. If $\Delta\mu = 0$, the net growth rate is zero, whereas for large (negative) $\Delta\mu$ the maximum growth rate is attained.

For colloidal suspensions we assume that Eq. (13) is applicable and that the maximum growth rate is determined by diffusion of single particles near the crystal surface. Using again the characteristic length scale l from Eq. (11), we obtain

$$v_m = \mathcal{B}\frac{D_s}{l}\tag{14}$$

where the prefactor $\mathcal{B}$ is expected to be $\mathcal{O}(1)$ and D_s is a self diffusion coefficient. Combination with Eq. (13) yields

$$v = \mathcal{B}\frac{D_s}{\sigma}\phi^{1/3}\left[1 - \exp(\Delta\mu/k_BT)\right].\tag{15}$$

The same procedure was followed by Russel, except that he used the estimate $l = \sigma$ [13]. For suspensions of charged colloidal particles, crystallizing at low volume fraction ($\phi < 0.001$), Eq. (15) was verified using direct observations [29]. For these particles, $D_s = D_0 \approx D_s^S$ was used.

It is not obvious which diffusion coefficient has to be used to describe growth of hard-sphere crystals. On the one hand, since it is assumed that diffusion has to

take place on a length scale $l > \sigma$, it seems appropriate to use the choice $D_s = D_s^L$. On the other hand, an important observation is that growth of heterogeneously nucleated crystals is found to proceed at concentrations above the glass transition, where $D_s^L = 0$ [24]. This again suggests that the growth kinetics are best expressed in terms of D_s^S, since short-time self diffusion is expected to remain non-zero at concentrations above the glass transition (see Section 2). In view of computer simulation results [30] it is conceivable that co-operative motions of particles near the crystal surface are important, and that therefore neither D_s^S nor D_s^L provide a good description of crystal growth. However, as a practical approach, we examine both choices $D_s = D_s^S$ and $D_s = D_s^L$.

4. Hard spheres

In this section we apply the theory presented in the preceding sections to calculate the nucleation rate and the growth rate of hard-sphere crystals. In order to calculate the nucleation rate from Eq. (12) expressions are needed for γ and $\Delta\mu$.

Firstly, we consider the surface free energy. A number of theoretical studies of the hard-sphere liquid-crystal interface have appeared, using different modifications of density functional theory. The most accurate theory available seems to be the one due to Curtin [31]. The values for the fcc (100) and (111) crystal planes differ little; we use the average $\gamma = 0.65\,k_BT/\sigma^2$. This value is also used in the metastable region and it is not corrected for the surface curvature. It is by no means clear that these assumptions are justified (see, for instance, Ref. [32]).

Secondly, we have to calculate $\Delta\mu$. We assume that, although the system is not at thermodynamic equilibrium, the nucleation takes place at mechanical equilibrium [13]. At the freezing concentration, $\phi = \phi_F$, the osmotic pressure of the initial fluid $\Pi_{liq} = \Pi_{coex}$, where the subscript denotes properties at coexistence. This fluid coexists with a solid with $\phi_{sol} = \phi_M$, the melting volume fraction. When a metastable fluid is prepared, $\phi > \phi_F$ and $\Pi_{liq} > \Pi_{coex}$. Due to this increased pressure the initially formed nucleus will have a volume fraction $\phi_{sol} > \phi_M$.

To calculate ϕ_{sol} we first have to specify equations of state, both for the fluid phase and for the solid phase. A good expression for the (metastable) liquid at high density is [33]

$$\frac{\Pi}{\rho k_B T} = \frac{3\phi_m}{\phi_m - \phi},$$ (16)

where we take $\phi_m = \phi_{rcp} = 0.64$. For the hard-sphere fcc crystal Eq. (16) can also be used, with $\phi_m = \phi_{fcc} = \pi/3\sqrt{2} \approx 0.74$ [34]. Using Eq. (16), both for the fluid phase and for the solid phase, ϕ_{sol} is obtained by solving

$$\Pi_{sol}(\phi_{sol}) - \Pi_{sol}(\phi_M) = \Pi_{liq}(\phi) - \Pi_{liq}(\phi_F).$$ (17)
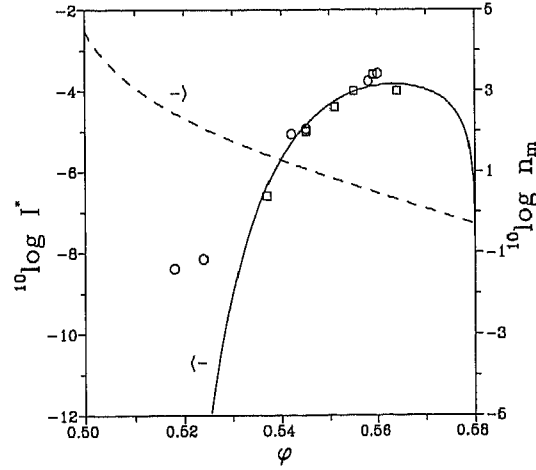
Figure 3. Calculated dimensionless nucleation rate I^* [solid line, Eq. (19)] and number of particles in the critical nucleus n_m [dashed line, Eq. (9)] for hard spheres. (O) Data I^* Schätzel and Ackerson with $\mathcal{A} = 10$ [35]. ($\square$) Data I^* Henderson, arbitrary units [36].

To calculate $\Delta\mu$, we use for each phase

$$\frac{\mu - \mu_{\text{coex}}}{k_B T} = \frac{1}{k_B T} \int_{\phi_{\text{coex}}}^{\phi} \left(\frac{\partial \mu}{\partial \phi}\right) d\phi = \frac{1}{k_B T} \int_{\phi_{\text{coex}}}^{\phi} \left(\frac{\partial \Pi}{\partial \rho}\right) \frac{d\phi}{\phi}. \tag{18}$$

After solving Eq. (18) for both phases using Eqs. (16) and (17), $\Delta\mu = \mu_{\text{sol}} - \mu_{\text{liq}}$ is calculated. At $\phi = \phi_F$, $\Delta\mu = 0$, and $\Delta\mu$ decreases continuously with increasing ϕ. At $\phi = 0.58$ we obtain $\Delta\mu = -2.5\ k_B T$. As crystallization proceeds, for the metastable liquid ϕ decreases, Π decreases, $\Delta\mu \rightarrow 0$, and therefore the crystallization kinetics will become time dependent. In the present discussion we neglect this effect.

From Eq. (12) we calculate a dimensionless nucleation rate

$$I^* \equiv \frac{I\sigma^5}{\mathcal{A} D_0} = \phi^{5/3}(1 - \phi/\phi_G)^{3\phi_G} \exp\left\{-\frac{4\pi^3(\gamma\sigma^2/k_B T)^3}{27\phi^2(\Delta\mu/k_B T)^2}\right\}. \tag{19}$$

The result for I^* and n_m is given in Figure 3. At $\phi \approx 0.57$, n_m becomes of order unity, so at high volume fraction the applicability of Eq. (19) becomes doubtful. The nucleation rate increases with ϕ until $\phi = 0.56$, due to the decrease of ΔG_m. At higher ϕ, I^* decreases again because D_s^L vanishes at ϕ_G. Russel [13] predicts a much more pronounced ϕ-dependence of I^*. The main cause for this discrepancy seems to be that he uses $\gamma = 4 k_B T/\sigma^2$.

Experimentally it is not obvious how I should be determined. The final crystallite number density, N_c, can be determined using light scattering experiments or by
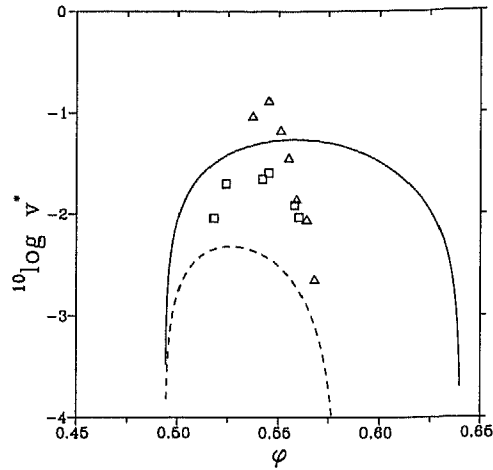
Figure 4. Calculated dimensionless crystal growth rate for hard spheres using $D_s = D_s^S$ (solid line) and $D_s = D_s^L$ (dashed line). ($\square$) Data Schätzel and Ackerson [35]. ($\triangle$) Data Henderson, arbitrary units [36].

direct counting. The question then is on what time scale these crystals have been formed. Recently, small-angle light scattering was used to study crystallization in hard-sphere dispersions [35]. The nucleation rate was estimated as N_c divided by t_c, the time needed for crystals to fill the sample, assuming that nucleation continues throughout the crystallization process. The results are included in Figure 3. Using $\mathcal{A} = 10$, the agreement with our prediction is reasonable. This agreement is perhaps fortuitous, but nevertheless it is encouraging that the predicted absolute nucleation rate seems reasonable.

Another set of experiments on hard-sphere dispersions, using light scattering at the main (111) Bragg reflection angle, was carried out by Henderson [36]. To calculate I he divides N_c by t_i, the induction time after which Bragg peaks become visible, assuming that nucleation takes place only at this initial stage. In Figure 3 the results (in arbitrary units) agree well with the prediction, spanning three decades in I.

Using Eq. (15) a dimensionless crystal growth rate is calculated,

$$v^* \equiv \frac{v\sigma}{\mathcal{B}D_0} = \frac{D_s}{D_0}\phi^{1/3}\left[1 - \exp(\Delta\mu/k_BT)\right], \tag{20}$$

where D_s is obtained from Eqs. (4) and (6). The results are shown in Figure 4. They depend rather much on the expression used for D_s. For $D_s = D_s^L$, v^* not only vanishes at a much lower ϕ, the maximum is also an order of magnitude smaller than for $D_s = D_s^S$.

Experimentally v can be measured directly using microscopy. For hard-sphere dispersions this does not seem to have been done. There is some experimental information available for v, however. Schätzel and Ackerson [35] interpret their results in terms of a diffusion-controlled growth model. They calculate a growth coefficient that does not seem to follow the behaviour of either of the two diffusion coefficients D_s. We use their data to calculate v as R_c/t_c, the typical crystal size at completion time divided by the completion time (in their notation). Putting $B = 1$ we obtain the results given in Figure 4. The order of magnitude of v^* is in between the two predictions. The concentration dependence resembles most the prediction using D_s^L.

We also include in Figure 4 results by Henderson [36]. He calculates v from the rate at which the Bragg peak intensity increases, yielding results in arbitrary units. His values decrease rather steeply with ϕ, even steeper than predicted using $D_s = D_s^L$.

5. Discussion

The use of colloidal suspensions as models to study crystallization has been demonstrated. A simple model has been presented to describe crystallization in hard-sphere suspensions. Although many assumptions had to be made in the derivation, this approach may be of help to understand crystallization kinetics in colloidal suspensions. Both for crystal nucleation and for crystal growth reasonable agreement with experimental observations is obtained.

Several assumptions were already mentioned above. In addition, it should be noted that crystal nucleation and crystal growth have been treated as if they were independent processes. In practice, both will compete and crystallization will therefore have a complex time dependence. Furthermore, the nucleation rate was calculated using a steady-state assumption. Starting from a homogeneous suspension a distribution of nucleus sizes will have to develop first. This will give rise to an induction time before nucleation actually begins. A first quantitative interpretation of such induction times in colloidal suspensions was given by Marr and Gast [37].

Another factor of experimental importance, that we have not discussed so far, is polydispersity. Colloidal suspensions are always somewhat polydisperse, a relative standard deviation of the particle size of $s = 0.05$ being fairly good. For hard spheres it is predicted, however, that crystallization will be suppressed when the polydispersity exceeds a critical value, in the range $0.045 < s < 0.11$ [6]. At $s = 0.075$ crystallization seemed to be significantly hindered already [6].

To conclude, in the past few years, the first detailed studies of crystallization kinetics in colloidal suspensions have appeared [29,36,38–41]. Such experiments, combined with a more sophisticated theoretical interpretation, can yield a wealth of information about the process of crystallization.

References

1. L. Onsager, Chem. Rev. 13 (1933) 73
2. W. G. McMillan and J. E. Mayer, J. Chem. Phys. 13 (1945) 276
3. N. A. M. Verhaegh and A. van Blaaderen, Langmuir 10 (1994) 1427
4. P. N. Pusey *et al.*, Phys. Rev. Lett. 63 (1989) 2753
5. P. Pieranski, Contemp. Phys. 24 (1983) 25
6. P. N. Pusey, in Liquids, Freezing and Glass Transition, Eds. J. P. Hansen, D. Levesque, and J. Zinn-Justin (Elsevier, Amsterdam, 1991), pp. 763–942
7. A. K. Sood, in Structural Ordering in Colloidal Suspensions, Vol. 45 of Solid State Physics, Eds. H. Ehrenreich and D. Turnbull (Academic, Boston, 1991), pp. 1–73
8. B. J. Alder and T. E. Wainwright, J. Chem. Phys. 27 (1957) 1208
9. W. G. Hoover and F. H. Ree, J. Chem. Phys. 49 (1968) 3609
10. P. N. Pusey and W. van Megen, in Physics of Complex and Supramolecular Fluids, Eds. S. A. Safran and N. A. Clark (Wiley, New York, 1987), pp. 673–698
11. W. van Megen and S. M. Underwood, Nature 362 (1993) 616
12. J. S. van Duijneveldt, Ph.D. thesis, Utrecht University, 1994
13. W. B. Russel, Phase Transitions 21 (1990) 127
14. G. K. Batchelor, J. Fluid Mech. 74 (1976) 1
15. B. Cichocki and B. U. Felderhof, J. Chem. Phys. 89 (1988) 1049
16. C. W. J. Beenakker and P. Mazur, Physica A 120 (1983) 388
17. P. N. Pusey and W. van Megen, J. Phys. (Paris) 44 (1983) 285
18. A. van Veluwen, H. N. W. Lekkerkerker, C. G. de Kruif, and A. Vrij, J. Chem. Phys. 87 (1987) 4873
19. R. J. Speedy, J. Chem. Phys. 100 (1994) 6684, and references therein
20. G. K. Batchelor, J. Fluid Mech. 131 (1983) 155
21. B. Cichocki and B. U. Felderhof, J. Chem. Phys. 89 (1988) 3705
22. E. Bartsch, V. Frenz, S. Möller, and H. Sillescu, Physica A 201 (1993) 363
23. A. van Blaaderen, J. Peetermans, G. Maret, and J. K. G. Dhont, J. Chem. Phys. 96 (1992) 4591
24. W. van Megen and S. M. Underwood, Phys. Rev. E 49 (1994) 4206
25. D. Turnbull and J. C. Fisher, J. Chem. Phys. 17 (1949) 71
26. R. F. Strickland-Constable, Kinetics and Mechanism of Crystallization (Academic, London, 1968)
27. H. A. Wilson, Philos. Mag. 50 (1900) 238
28. J. Frenkel, Phys. Z. Sowjetunion 1 (1932) 498
29. D. J. W. Aastuen, N. A. Clark, L. K. Cotter, and B. J. Ackerson, Phys. Rev. Lett. 57 (1986) 1733
30. E. Burke, J. Q. Broughton, and G. H. Gilmer, J. Chem. Phys. 89 (1988) 1030
31. W. A. Curtin, J. Chem. Phys. 39 (1989) 6775
32. D. W. Oxtoby, Adv. Chem. Phys. 70 (1988) 263
33. L. V. Woodcock, Ann. N. Y. Acad. Sci. 371 (1981) 274
34. K. R. Hall, J. Chem. Phys. 57 (1972) 2252
35. K. Schätzel and B. J. Ackerson, Phys. Rev. E 48 (1993) 3766
36. S. Henderson, Crystallization Mechanisms in Colloidal Systems, 1993, B. Sc. thesis, Royal Melbourne Institute of Technology
37. D. W. Marr and A. P. Gast, Langmuir 10 (1994) 1348
38. K. Schätzel and B. J. Ackerson, Phys. Rev. Lett. 68 (1992) 337
39. J. K. G. Dhont, C. Smits, and H. N. W. Lekkerkerker, J. Colloid Interface Sci. 152 (1991) 386
40. D. J. W. Aastuen, N. A. Clark, J. C. Swindal, and C. D. Muzny, Phase Transitions 21 (1990) 139
41. D. G. Grier and C. A. Murray, J. Chem. Phys. 100 (1994) 9088